SIAM J. Appl. Math.
Vol. 74, No. 3, pp. 697–723

ASYMPTOTIC AND NUMERICAL SOLUTIONS OF A FREE BOUNDARY PROBLEM FOR THE SORPTION OF A FINITE AMOUNT OF SOLVENT INTO A GLASSY POLYMER*

S. L. MITCHELL†‡ and S. B. G. O'BRIEN†

Abstract. The behavior of the one-phase Stefan problem describing the sorption of a finite amount of swelling solvent is studied. The solvent diffuses into the polymer, which causes it to change from a glassy to a rubbery state. The interface between these two states is characterized by a moving boundary, whose speed is defined by a kinetic law. A key distinctive feature of the model in this paper is that the polymer is exposed initially to a finite amount of penetrant and eventually approaches an equilibrium value. This equilibrium causes the time history of the interface to be more complex than that of the related, and more studied, problem where the swelling process occurs instantaneously at the penetration surface. We analyze the model using formal asymptotic expansions, for both small and large times as well as for the large control parameter. A numerical scheme is described which immobilizes the boundary and correctly identifies the appropriate starting solution. In addition, we discuss the heat balance integral method applied to this system and show that, while it does not give a particularly accurate approximation of the concentration, it is very good at capturing the behavior of the moving boundary position and also helps motivate our large time expansion. The form of the kinetic law is usually assumed to be linear, but this is a nonphysical restriction, and we are able to determine accurate asymptotic and numerical results for the nonlinear case.

Key words. solvent drug penetration, asymptotics, Stefan problem, Keller box scheme, heat balance integral method, artificial parameter

AMS subject classifications. 35B20, 35G31, 65N06, 40C10, 35K05

DOI. 10.1137/120899200

1. Introduction.

A widespread problem in the pharmaceutical industry is how to combine an active agent (the solvent) with its carrier (a polymer) in the most appropriate and economical manner. The drug release mechanism is categorized as a diffusive process [7], and the resulting devices can eliminate or greatly alleviate problems associated with conventional usage of pharmaceuticals, such as systemic effects, patient compliance, and inaccurate dosages. (A comprehensive review of models describing solvent penetration into polymers can be found in [2].)

We assume that the polymer starts out in a dry glassy state and is then immersed into a solvent. Provided that the amount of solvent is above a certain threshold value, the solvent will diffuse into the polymer, transforming the affected region into a rubbery phase. The glassy-rubbery interface is described by a moving boundary whose kinetics is governed by an empirical law relating the concentration of solvent at that point to the velocity of the interface, as discussed in [1, 4, 5, 6, 12, 14]. The presence of a moving boundary means that the system can be thought of as a one-dimensional Stefan problem [8], which usually refers to the melting or solidification of a material.

*Received by the editors November 16, 2012; accepted for publication (in revised form) February 19, 2014; published electronically May 29, 2014. This work was supported by MACSI, the Mathematics Applications Consortium for Science and Industry (www.macsi.ul.ie), funded by the Science Foundation Ireland Mathematics Initiative grant 06/MI/005.

http://www.siam.org/journals/siap/74-3/89920.html

†Mathematics Applications Consortium for Science and Industry (MACSI), Department of Mathematics and Statistics, University of Limerick, Limerick, Ireland (sarah.mitchell@ul.ie, stephen.obrien@ul.ie).

‡Corresponding author.

The key features of the model for diffusion of glassy polymers are very similar since they also involve a nonlinear boundary value problem where the phase-change boundary moves with time and its location is unknown in advance. The analogue of the threshold value would be the melting temperature. The diffusion polymer problem can also be categorized as a generalized Stefan problem which includes kinetic undercooling at the moving boundary [10, 11]. The kinetic condition associates interface undercooling with interface growth rate, which is characterized by a dependence of the velocity of the phase-change boundary on the phase-change temperature.

In this present work we consider the one-dimensional free boundary problem describing the sorption of a *finite* amount of penetrant into a glassy polymer [5]. This is in contrast to a similar problem where the swelling process occurs instantaneously at the penetration surface [5, 17]. A zero flux boundary condition is maintained at $x = 0$, and the solvent-polymer system approaches an equilibrium value at $u = u^*$, where u is the concentration of the solvent. The equilibrium causes the time history of the interface to be more complex than that of the related problem considered in [5, 17]. Another difference is that the initial position of the moving front is positive. This requires an initial condition to be specified for u, and for simplicity we assume that it is constant.

Numerically speaking, the finite problem may seem no harder than the other problem considered in [5, 17]. However, there are different issues that arise in the attempt to produce a numerical scheme that is second-order accurate in both time and space. We follow Mitchell et al. [19], who solve a moving boundary problem for the transient heating of an evaporating spherical droplet using the Keller box finite-difference scheme [18]. In that problem the solution domain is initially finite in extent and subsequently shrinks as the droplet evaporates. A similar approach can be carried out here, and, in order to obtain a self-consistent asymptotic structure as $t \to 0^+$, we must make a similarity transformation for the space variable, which leads to an infinite spatial domain in this limit. Fortunately this adds little complication to the computation, and we are able to obtain a numerical scheme that is second-order accurate in time and space for all variables, as demonstrated in [19].

An important feature of the model is the precise form of the kinetic law, as this greatly affects the asymptotic structure of the solutions in different limits. It is usually assumed to be a power-law form such as $(u - u^*)^n$—see [3, 11], for example—and most authors use a linear relationship to simplify the subsequent analysis [5, 14, 17]. However, the power typically lies in the range $2 < n \leq 3$, and so we keep this power general for most of the study [3].

This precise problem has only been studied before by Cohen and Erneux [5], and their scaling leads to a form that is not easy to compare with related models. We choose a scaling which is consistent with the problem in [17] and consider asymptotic limits of small and large time as well as large control parameter. We give a detailed analysis of these limits and obtain accurate high-order terms which are compared to numerical results. The asymptotic structure is more complicated here, and we find that boundary layers arise for the small time and large control parameter expansions. In addition, the fact that the solution eventually approaches an equilibrium value causes the time history of the interface to be complicated, and we cannot determine a closed form solution for the large time expansion. However, patching with the numerical solution leads to very accurate results for times right down to $\mathcal{O}(1)$.

In addition, we discuss the application to this problem of the heat balance integral method (HBIM), which is a popular approximate solution method for solving thermal

and Stefan problems [13, 15, 16, 22]. The method involves assuming an approximating function for the temperature, typically a polynomial, and then integrating the heat equation over the spatial domain. This reduces the problem to solving a set of first-order ODEs, which often have analytic solutions. For the diffusion polymer model we can define an approximating function for the concentration in the same way [17]. An alternative approach to the HBIM is the refined integral method (RIM), where the heat equation is integrated twice [15, 23]. Recently, Mitchell and Myers [16, 22] have developed a method where the exponent in the approximating polynomial is determined during the solution process, producing significantly better results than previous heat balance methods. However, the combined integral method (CIM) turns out to be more complicated for this problem, where the polymer is exposed initially to a finite amount of penetrant. We instead use the classic HBIM but with the exponent found using the Myers minimization method [20, 21]. Although this approach does not give a particularly accurate approximation of the solvent concentration, it does very well at predicting the behavior of the moving boundary position and also helps motivate our large time expansion, which is usually of more practical interest. The unsatisfactory results for the concentration are not particularly surprising, since it has been noted by Crank and Gupta [9] that heat balance integral methods are not especially accurate in cases of nonzero initial distributions with zero flux boundary conditions.

The structure of the paper is as follows. In section 2 we formulate the governing equations describing the one-dimensional finite polymer diffusion model. A numerical method is described in section 3, and we discuss a transformation to immobilize the boundary and perform an analysis in the small time limit, which is necessary for the numerical solution. This numerical solution is used throughout the paper as a benchmark for testing the accuracy of the approximate solutions. In section 4 we discuss the heat balance integral method and perform a large time expansion of the resulting ODE, which helps to guide our large time asymptotic analysis of the full model. In sections 5, 6, and 7 we analyze the asymptotic limits of small and large time and large control parameter, respectively, and compare these results with the numerical solution. Finally, in section 8 we draw some conclusions.

2. Mathematical formulation. The mathematical problem concerns a slab of glassy polymer that is in contact with a solvent [5]. If the solvent concentration exceeds some threshold value, then the solvent moves into the polymer, creating a swollen layer in which the solvent diffuses according to Fick's second law of diffusion. The boundary between the swollen region and the glassy region obeys an empirical penetration law, relating its velocity to the solvent concentration at that point. An additional condition on the free boundary is obtained by imposing mass conservation, i.e., equating the mass density to the product of the solvent concentration and the velocity of the free boundary. The problem is given by

$$\frac{\partial u}{\partial t} = D\frac{\partial^2 u}{\partial x^2}, \qquad 0 < x < s(t), \tag{2.1}$$

$$\frac{\partial u}{\partial x} = 0 \qquad \text{at } x = 0, \tag{2.2}$$

$$(u + k_1)\frac{\mathrm{d}s}{\mathrm{d}t} = -D\frac{\partial u}{\partial x} \qquad \text{at } x = s(t), \tag{2.3}$$

$$\frac{\mathrm{d}s}{\mathrm{d}t} = k_2(u - u^*)^n \qquad \text{at } x = s(t), \tag{2.4}$$

$$s(0) = s_i \neq 0, \qquad u(x, 0) = u_i\,. \tag{2.5}$$

Equation (2.1) is Fick's diffusion law for a one-dimensional system, and the condition (2.4) is the penetration law describing the swelling kinetics; i.e., there is a threshold value u^*, and above this value the interface moves with a speed given by a power law with index n. Thus k_2 and n are phenomenological quantities. It is common to assume a linear relationship [14, 17] in the kinetic law (2.4), but, as discussed in the introduction, we leave it as a general exponent in the analysis that follows. Finally, (2.3) gives the mass balance at the moving front. It is derived by assuming that the flux from the swelling region across the moving boundary, given by $-Du_x - us_t$, is proportional to the flux generated by the interface region. Thus

$$-D\frac{\partial u}{\partial x} - u\frac{\mathrm{d}s}{\mathrm{d}t} = K(u-u^*)^n \qquad \text{at } x = s(t)\,,$$

and combining this with (2.4) gives (2.3), where $k_1 = K/k_2$.

Before nondimensionalizing these equations it is useful to note that the boundary condition (2.2) allows us to derive a conservation relation which is more widely used [5] than the boundary condition (2.3). Suppose we integrate (2.1) with respect to x over the domain; i.e.,

$$\int_0^s u_t \,\mathrm{d}x = Du_x\big|_{x=s} - Du_x\big|_{x=0}\,. \tag{2.6}$$

After applying the Leibniz rule and boundary condition (2.2), this reduces to

$$\frac{\mathrm{d}}{\mathrm{d}t}\int_0^s u\,\mathrm{d}x - u\big|_{x=s}s_t = Du_x\big|_{x=s}\,. \tag{2.7}$$

Replacing the right-hand side with (2.3), integrating, and using the initial conditions in (2.5), we find

$$\int_0^s u\,\mathrm{d}x + k_1 s = (u_i + k_1)s_i\,. \tag{2.8}$$

Combining this equation with (2.1)–(2.4), it follows that the equilibrium solution is

$$u = u^*\,, \qquad s = \frac{(u_i+k_1)s_i}{u^*+k_1}\,. \tag{2.9}$$

The problem can be nondimensionalized by setting

$$x' = \frac{x}{X}\,, \qquad t' = \frac{t}{T}\,, \qquad u' = \frac{u-u^*}{\Delta u}\,, \qquad s' = \frac{s}{X}\,, \tag{2.10}$$

where $\Delta u = u_i - u^*$. Cohen and Erneux [5] chose the time-scale from (2.4) and used the conservation relation (2.8) to determine the length-scale, by balancing the integral term with the right-hand side. Their main focus was in examining the limit $s_i \to 0$, and their scaling led to parameters which easily quantified this. In fact, x and s could also be scaled with s_i or even the equilibrium solution. Their formulation gives rise to an $\mathcal{O}(1)$ parameter in the diffusion equation, but we prefer to choose T to balance the diffusion equation, leading to $T = X^2/D$, and then set $X = s_i$ [14, 17]. Equations

(2.1)–(2.5) simplify (after dropping the $(\cdot)'$ notation) to

$$\frac{\partial u}{\partial t} = \frac{\partial^2 u}{\partial x^2}\,, \qquad 0 < x < s(t), \tag{2.11}$$

$$\frac{\partial u}{\partial x} = 0 \qquad \text{at } x = 0, \tag{2.12}$$

$$(\lambda + u)\frac{\mathrm{d}s}{\mathrm{d}t} = -\frac{\partial u}{\partial x} \qquad \text{at } x = s(t), \tag{2.13}$$

$$\mu\frac{\mathrm{d}s}{\mathrm{d}t} = u^n \qquad \text{at } x = s(t), \tag{2.14}$$

$$s = 1 \text{ and } u = 1 \qquad \text{at } t = 0\,, \tag{2.15}$$

where λ and μ are the control and kinetic parameters, respectively, defined by

$$\lambda = \frac{u^* + k_1}{\Delta u}\,, \qquad \mu = \frac{D}{k_2 s_i \Delta u^n}\,. \tag{2.16}$$

Note that λ is analogous to a Stefan number and typically varies from $\mathcal{O}(1)$ to large, whereas μ is often small [14], but we will allow some latitude in our analysis. Observe from (2.16) that λ and μ both contain Δu in the denominator, and so if the initial value u_i is close to the threshold value u^*, then both of these parameters could be large.

The conservation relation (2.8) is now

$$\int_0^s u\,\mathrm{d}x + \lambda s = 1 + \lambda\,, \tag{2.17}$$

and the equilibrium solution (2.9) becomes

$$u = 0\,, \qquad s = 1 + \frac{1}{\lambda}\,. \tag{2.18}$$

3. Numerical solution. For the numerical solution it is convenient to immobilize the boundary by setting

$$\xi = \frac{x}{s}\,, \qquad u(x,t) = 1 + sF(\xi,t)\,. \tag{3.1}$$

Note that we could have simply used $u(x,t) = F(\xi,t)$; since $s(0) = 1$, there is no issue with dividing by s for small times, but the formulation in (3.1) leads to a neater transformation. Then (2.11)–(2.15) become

$$\frac{\partial^2 F}{\partial \xi^2} = s^2\frac{\partial F}{\partial t} + ss_tF - \xi ss_t\frac{\partial F}{\partial \xi}\,, \quad 0 < \xi < 1, \tag{3.2}$$

$$\frac{\partial F}{\partial \xi} = 0 \qquad \text{at } \xi = 0, \tag{3.3}$$

$$\frac{\partial F}{\partial \xi} = -(\lambda + 1 + sF)\frac{\mathrm{d}s}{\mathrm{d}t} \qquad \text{at } \xi = 1, \tag{3.4}$$

$$\mu\frac{\mathrm{d}s}{\mathrm{d}t} = (1 + sF)^n \qquad \text{at } \xi = 1, \tag{3.5}$$

$$s = 1 \text{ and } F = 0 \qquad \text{at } t = 0\,. \tag{3.6}$$

We seek a self-consistent asymptotic structure for the solution to these equations as $t \to 0^+$. Whereas the solution $s = 1 + t/\mu$, $F = 0$ is compatible with (3.5) and (3.6), it is not compatible with (3.4). Thus we follow [19] and set

$$\eta = \frac{1-\xi}{\sqrt{t}}\,, \qquad \zeta = \sqrt{t}\,, \qquad F(\xi,t) = \zeta G(\eta,\zeta)\,. \tag{3.7}$$

Then (3.2)–(3.5) become

$$2\frac{\partial^2 G}{\partial \eta^2} = s^2\left(G + \zeta\frac{\partial G}{\partial \zeta} - \eta\frac{\partial G}{\partial \eta}\right) + \zeta s s_\zeta G + (1-\eta\zeta)s s_\zeta \frac{\partial G}{\partial \eta}, \quad 0 < \eta < 1/\zeta, \tag{3.8}$$

$$\frac{\partial G}{\partial \eta} = 0 \qquad \text{at } \eta = 1/\zeta, \tag{3.9}$$

$$2\zeta\frac{\partial G}{\partial \eta} = (\lambda + 1 + s\zeta G)\frac{\mathrm{d}s}{\mathrm{d}\zeta} \qquad \text{at } \eta = 0, \tag{3.10}$$

$$\mu\frac{\mathrm{d}s}{\mathrm{d}\zeta} = 2\zeta(1+s\zeta G)^n \qquad \text{at } \eta = 0\,, \tag{3.11}$$

with $s(0) = 1$, and this combined with (3.11) implies that $s \sim 1 + \zeta^2/\mu$ as $\zeta \to 0^+$. In order to determine an initial condition for the system (3.8)–(3.11), we consider the limit as $\zeta \to 0^+$. Then (3.8)–(3.10) reduce to the second-order ODE

$$2G''(\eta) = G(\eta) - \eta G'(\eta)\,, \qquad G'(\eta)\big|_{\eta\to\infty} \to 0\,, \qquad G'(0) = \frac{\lambda+1}{\mu}\,, \tag{3.12}$$

which has solution

$$G(\eta) = \frac{\lambda+1}{\mu}\left[\eta\,\mathrm{erfc}\left(\frac{\eta}{2}\right) - \frac{2}{\sqrt{\pi}}\exp\left(-\frac{\eta^2}{4}\right)\right]\,, \tag{3.13}$$

where $\mathrm{erfc}\,(x)$ is the complementary error function. The full system (3.8)–(3.11) can now be solved numerically using the Keller box scheme along with the initial condition (3.13). This is described in more detail in [17, 19]. In practice, a finite computational domain of extent η_∞ is chosen, and (3.8)–(3.11) and (3.13) are solved for $0 \le \zeta \le \zeta^*$, where $\zeta^* = 1/\eta_\infty$. Subsequently, for $\zeta > \zeta^*$, the numerical integration is continued in (ξ,ζ) variables, i.e., by solving (3.2)–(3.5) but after making the transformation $\zeta = \sqrt{t}$, using the solution at $\zeta = \zeta^*$ as the initial condition. The discretization parameters used throughout the paper are $\eta_\infty = 10$, $\Delta\tau = 0.02$, $\Delta\eta = 0.4$, and $\Delta\xi = 0.04$.

4. Heat balance integral method. In this section we apply the classic HBIM to (2.1)–(2.5). Mitchell and O'Brien [17] analyzed a variant of this method, called the combined integral method (CIM), for the related problem where the swelling process occurs instantaneously at the penetration surface and its initial thickness is zero. The CIM is generally more accurate than the HBIM, but it turns out to be more complicated when the polymer is exposed initially to a finite amount of penetrant. For the problem presented in this paper we shall show that while these methods are less accurate here than when applied to the problem in [17], the resulting equations are useful for corroborating the correct balances for the large time asymptotic solution in section 6. For a full discussion of the HBIM and RIMs, see [15, 17, 21, 22] and references therein.

We approximate u with the polynomial form

$$u(x,t) = a + b\left(1 - \frac{x}{s}\right) + c\left(1 - \frac{x}{s}\right)^m , \tag{4.1}$$

where a, b, c are possibly time dependent and $m > 1$. Noting that (2.13) and (2.14) can be combined to eliminate the $\mathrm{d}s/\mathrm{d}t$ term, we use this and (2.12) to obtain

$$u = a + \frac{(\lambda + a)a^n s}{\mu}\left(1 - \frac{x}{s}\right) - \frac{(\lambda + a)a^n s}{\mu m}\left(1 - \frac{x}{s}\right)^m . \tag{4.2}$$

The boundary condition (2.14) gives the ODE $\mu s_t = a^n$. Since both a and s are unknown, the HBIM involves integrating the heat equation (2.11) over the domain $x \in [0,\, s]$ to obtain an extra equation, which is precisely the nondimensional version of (2.7). In contrast to classic Stefan problems, we can integrate to obtain the conservation relation (2.17). Substituting in u from (4.2) leads to the nonlinear equation

$$as + \frac{(m^2 + m - 2)(\lambda + a)a^n s^2}{2\mu m(m+1)} + \lambda s = 1 + \lambda\,. \tag{4.3}$$

Note that when $n = 1$, this is simply a quadratic expression for a, which can be solved to give a in terms of s. Then s is determined from the ODE $\mu s_t = a^n$. For $n \neq 1$ we must solve the coupled ODE-algebraic system for a and s.

The classic HBIM uses $m = 2$ to give a quadratic polynomial for u, but recently Mitchell and Myers (see [16, 20, 21, 22]) have shown that great improvements can be made if the exponent is left unknown and determined as part of the solution process. One option is to choose the exponent to minimize the Langford error [20, 21], and another is to combine the HBIM with the RIM, which gives an extra equation. This is the aforementioned CIM [16, 17, 22]. Here we apply the HBIM to (2.1)–(2.5), with m found using the Myers minimization method [20, 21]. The CIM approach leads to a time dependent m which further complicates the analysis and does not noticeably improve the accuracy.

Figures 1 and 2 present results for the HBIM solution compared with the numerical solution for various values of λ and two values of n. In the left-hand plots we show s against t, and we can see that the solutions are very accurate. However, the plots of u against x (right-hand plots) are not as good, which is due to specifying a zero flux at the left boundary. In [17] the authors consider the related problem where the swelling process occurs instantaneously at the penetration surface. This has a fixed concentration specified at $x = 0$, and there the HBIM gives accurate results for both u and s.

Despite the unsatisfactory results for u, the HBIM can prove useful in corroborating the large time behavior of the original equations. Let us consider a large time asymptotic approximation to the HBIM. Suppose we set

$$t = g(\varepsilon) + \varepsilon^\gamma \tau\,, \qquad s(t) = 1 + \frac{1}{\lambda} + \varepsilon^\alpha S(\tau)\,, \qquad a(t) = \varepsilon^\beta A(t)\,, \tag{4.4}$$

where $\varepsilon \ll 1$ is an artificial parameter and $g(\varepsilon) \gg 1$, to be determined, is the relevant time-scale over which u decays to $\mathcal{O}(\varepsilon)$. Then the ODE $\mu s_t = a^n$ becomes

$$\mu\varepsilon^{\alpha-\gamma} S_\tau = \varepsilon^{n\beta} A^n\,, \tag{4.5}$$

which shows that $\alpha - \gamma = n\beta$. The nonlinear equation (4.3) is now

$$\varepsilon^\beta A\left(1 + \frac{1}{\lambda} + \varepsilon^\alpha S\right) + \frac{(m^2 + m - 2)}{2\mu m(m+1)}(\lambda + \varepsilon^\beta A)\varepsilon^{n\beta} A^n \left(1 + \frac{1}{\lambda} + \varepsilon^\alpha S\right)^2 + \lambda\varepsilon^\alpha S = 0. \tag{4.6}$$

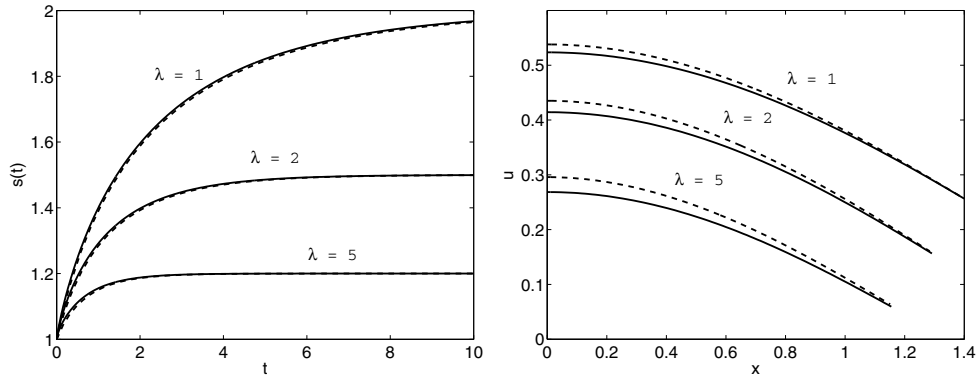

FIG. 1. *Comparison of numerical (solid line) and HBIM (dashed line) solutions. Left: s against t. Right: u against x (at t = 1) for μ = n = 1 and various values of λ. Values of m are* 2.5836, 2.6078, 2.6588, *for λ = 1, 2, 5, respectively.*

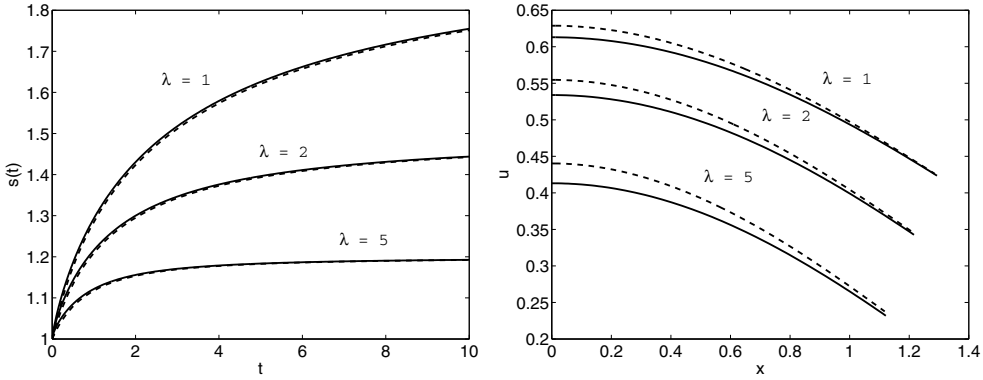

FIG. 2. *Comparison of numerical (solid line) and the HBIM (dashed line) solutions. Left: s against t. Right: u against x (at t = 1) for μ = 1, n = 2, and various values of λ. Values of m are* 2.5492, 2.5582, 2.5792, *for λ = 1, 2, 5, respectively.*

The balance must come from the first and last terms, which show that $\beta = \alpha$. Therefore, since we are free to choose one exponent, it is simplest to set $\alpha = \beta = 1$, which gives $\gamma = 1 - n$, and so the time-scale is $t = g(\varepsilon) + \varepsilon^{1-n}\tau$.

Thus, for $n = 1$ we simply have $t = g(\varepsilon) + \tau$, and (4.6) reduces to

$$A\left(1 + \frac{1}{\lambda}\right) + \frac{(m^2 + m - 2)}{2\mu m(m+1)}\lambda A\left(1 + \frac{1}{\lambda}\right)^2 + \lambda S = 0 \tag{4.7}$$

or

$$A = -kS\,, \qquad k = \frac{\lambda}{(1 + 1/\lambda) + \frac{(m^2+m-2)}{2\mu m(m+1)}\lambda(1 + 1/\lambda)^2}\,. \tag{4.8}$$

Then (4.5) is simply $\mu S_\tau = A$, which has solution $S = C\exp\left(-\frac{k\tau}{\mu}\right)$, with C being an undetermined coefficient. Back in the original variables we therefore have

$$s = 1 + \frac{1}{\lambda} + \varepsilon\, C \exp\left(-\frac{k(t - g(\varepsilon))}{\mu}\right)\,. \tag{4.9}$$

We must choose $g(\varepsilon)$ to eliminate the artificial parameter, i.e., by setting $\varepsilon e^{kg(\varepsilon)/\mu} = 1$. Thus the time-scale when $n = 1$ is $g(\varepsilon) = -\mu \ln \varepsilon / k$.

For $n > 1$ it follows that $t = g(\varepsilon) + \varepsilon^{1-n}\tau$, and the leading-order terms in (4.6) give $A = \lambda^2 S/(1+\lambda)$. Then the ODE for S is

$$\mu S_\tau = \left(-\frac{\lambda^2 S}{1+\lambda}\right)^n , \tag{4.10}$$

which has the general solution

$$S = -\frac{1}{\lambda^2}\left(\frac{\mu(1+\lambda)^n}{C + (n-1)\lambda^2\tau}\right)^{\frac{1}{n-1}} . \tag{4.11}$$

Expressing s in the original variables, we see that

$$\begin{aligned} s &= 1 + \frac{1}{\lambda} - \frac{\varepsilon}{\lambda^2}\left(\frac{\mu(1+\lambda)^n}{C + (n-1)\lambda^2\varepsilon^{n-1}(t - g(\varepsilon))}\right)^{\frac{1}{n-1}} \\ &= 1 + \frac{1}{\lambda} - \frac{1}{\lambda^2}\left(\frac{\mu(1+\lambda)^n}{F + (n-1)\lambda^2\varepsilon^{n-1}t}\right)^{\frac{1}{n-1}} , \end{aligned} \tag{4.12}$$

with $g(\varepsilon)$ chosen so that $F = \varepsilon^{1-n}C - (n-1)\lambda^2 g(\varepsilon)$.

Note that since $a = \varepsilon A$, it follows from examining (4.2) that u must also be scaled with ε, which we will need in our large time asymptotic analysis of the original system, as discussed in section 6.

5. Small time solution. Cohen and Erneux [5] consider only the limit $s_i \to 0$, but here we are interested in both small- and large time asymptotic solutions. While we could perform an asymptotic analysis of the governing equations after immobilizing the boundary, as was done by [5] for their related problem describing a constant reservoir of swelling solvent, we follow [17] and consider (2.11)–(2.15) directly.

To investigate a small time solution for λ, $\mu = \mathcal{O}(1)$ we set

$$t = \varepsilon\tau\,, \qquad u(x,t) \sim 1 + \sqrt{\varepsilon}\, v(x,\tau)\,, \qquad s(t) = 1 + \varepsilon L(\tau)\,, \tag{5.1}$$

where v, $L = \mathcal{O}(1)$ and $\varepsilon \ll 1$ is an artificial parameter. Then (2.11)–(2.14) become

$$\frac{\partial v}{\partial \tau} = \varepsilon \frac{\partial^2 v}{\partial x^2}\,, \qquad 0 < x < 1 + \varepsilon L, \tag{5.2}$$

$$\frac{\partial v}{\partial x} = 0 \qquad \text{at } x = 0, \tag{5.3}$$

$$(\lambda + 1 + \sqrt{\varepsilon} v)\frac{\mathrm{d}L}{\mathrm{d}\tau} = -\sqrt{\varepsilon}\frac{\partial v}{\partial x} \qquad \text{at } x = 1 + \varepsilon L, \tag{5.4}$$

$$\mu \frac{\mathrm{d}L}{\mathrm{d}\tau} = (1 + \sqrt{\varepsilon} v)^n \qquad \text{at } x = 1 + \varepsilon L, \tag{5.5}$$

$$L = 0 \text{ and } v = 0 \qquad \text{at } \tau = 0\,. \tag{5.6}$$

The outer solution for the concentration is $v = 0$. Boundary condition (5.5) gives $L = \tau/\mu$ at leading order, but this cannot satisfy the boundary condition (5.4), and so it follows that there must be a boundary layer at the right-hand edge. To incorporate this we rescale x as

$$x = 1 + \varepsilon L - \sqrt{\varepsilon} y\,, \qquad v(x,\tau) = w(y,\tau)\,. \tag{5.7}$$

Then the system becomes

$$\frac{\partial w}{\partial \tau} + \sqrt{\varepsilon}\frac{\mathrm{d}L}{\mathrm{d}\tau}\frac{\partial w}{\partial y} = \frac{\partial^2 w}{\partial y^2}\,, \qquad 0 < y < \infty, \tag{5.8}$$

$$(\lambda + 1 + \sqrt{\varepsilon}w)\frac{\mathrm{d}L}{\mathrm{d}\tau} = \frac{\partial w}{\partial y} \qquad \text{at } y = 0, \tag{5.9}$$

$$\mu\frac{\mathrm{d}L}{\mathrm{d}\tau} = (1 + \sqrt{\varepsilon}w)^n \qquad \text{at } y = 0, \tag{5.10}$$

$$w \to 0 \qquad \text{as } y \to \infty. \tag{5.11}$$

The condition (5.11) comes from matching the $x = 0$ boundary (now transformed to $y \to \infty$) with the outer solution $v = 0$.

It should be noted that if the boundary condition $\frac{\partial u}{\partial x} = 0$ did not agree with the initial condition $u(x, 0) = 1$, there would also be a boundary layer at $x = 0$ for small times. If $u(x, 0) = f(x)$ for arbitrary $f(x)$, then the solution would not be $u \sim 1$ to all orders. We could represent the initial condition as an asymptotic series, i.e.,

$$u(x,t) \sim u(x,0) + t\frac{\partial u}{\partial t}(x,0) + \frac{t^2}{2!}\frac{\partial^2 u}{\partial t^2}(x,0) + \cdots\,,$$

which shows the structure and highlights the fact that this equals 1 only when $f(x) = u(x, 0) \equiv 1$.

We now expand w and L in a series expansion by setting

$$w = w_0 + \sqrt{\varepsilon}w_1 + \cdots\,, \qquad L = L_0 + \sqrt{\varepsilon}L_1 + \cdots\,. \tag{5.12}$$

Thus at leading order (5.8)–(5.11) reduce to

$$\frac{\partial w_0}{\partial \tau} = \frac{\partial^2 w_0}{\partial y^2}, \qquad 0 < y < \infty, \tag{5.13}$$

$$(\lambda + 1)\frac{\mathrm{d}L_0}{\mathrm{d}\tau} = \frac{\partial w_0}{\partial y} \qquad \text{at } y = 0, \tag{5.14}$$

$$\mu\frac{\mathrm{d}L_0}{\mathrm{d}\tau} = 1 \qquad \text{at } y = 0, \tag{5.15}$$

$$w_0 \to 0 \qquad \text{as } y \to \infty. \tag{5.16}$$

The boundary condition (5.15) can immediately be integrated to give $L_0 = \tau/\mu$. For w_0 we have a similarity solution $w_0 = \sqrt{\tau}f_0(r)$, where $r = y/[2\sqrt{\tau}]$ and f_0 satisfies

$$\frac{1}{4}f_0''(r) + \frac{1}{2}rf_0'(r) - \frac{1}{2}f_0(r) = 0\,, \tag{5.17}$$

with boundary conditions

$$f_0(r)\big|_{r\to\infty} \to 0\,, \qquad f_0'(0) = \frac{2(\lambda+1)}{\mu}\,. \tag{5.18}$$

This has the solution

$$f_0(r) = \frac{2(\lambda+1)}{\mu}\left[r\,\mathrm{erfc}(r) - \frac{1}{\sqrt{\pi}}e^{-r^2}\right], \tag{5.19}$$

and so

$$w_0(y,\tau) = \frac{\lambda+1}{\mu}\left[y\,\mathrm{erfc}\left(\frac{y}{2\sqrt{\tau}}\right) - 2\sqrt{\frac{\tau}{\pi}}\exp\left(-\frac{y^2}{4\tau}\right)\right]. \tag{5.20}$$

Note that this agrees with the small time analysis carried out in section 3 to determine the initial condition (3.13) for the numerical scheme.

The $\mathcal{O}(\sqrt{\varepsilon})$ terms are

$$\frac{\partial w_1}{\partial \tau} + \frac{\mathrm{d}L_0}{\mathrm{d}\tau}\frac{\partial w_0}{\partial y} = \frac{\partial^2 w_1}{\partial y^2}, \qquad 0 < y < \infty, \tag{5.21}$$

$$(\lambda+1)\frac{\mathrm{d}L_1}{\mathrm{d}\tau} + w_0\frac{\mathrm{d}L_0}{\mathrm{d}\tau} = \frac{\partial w_1}{\partial y} \qquad \text{at } y = 0, \tag{5.22}$$

$$\mu\frac{\mathrm{d}L_1}{\mathrm{d}\tau} = n w_0 \qquad \text{at } y = 0, \tag{5.23}$$

$$w_1 \to 0 \qquad \text{as } y \to \infty. \tag{5.24}$$

Substituting w_0 into (5.23) leads to

$$L_1 = -\frac{4n(\lambda+1)\tau^{3/2}}{3\mu^2\sqrt{\pi}}. \tag{5.25}$$

For w_1 we have a similarity solution $w_1 = \tau f_1(r)$, where f_1 satisfies

$$\frac{1}{4}f_1''(r) + \frac{1}{2}r f_1'(r) - f_1(r) = \frac{(\lambda+1)\,\mathrm{erfc}(r)}{\mu^2}, \tag{5.26}$$

with boundary conditions

$$f_1(r)\big|_{r\to\infty} \to 0, \qquad f_1'(0) = -\frac{4(\lambda+1)\big[1+n(\lambda+1)\big]}{\mu^2\sqrt{\pi}}. \tag{5.27}$$

This has the solution

$$\begin{aligned} f_1(r) = {} & \frac{(\lambda+1)\big[1+n(\lambda+1)\big]}{\mu^2}\left[2\left(\frac{1}{2}+r^2\right)\mathrm{erfc}(r) - \frac{2r}{\sqrt{\pi}}e^{-r^2}\right] \\ & - \frac{\lambda+1}{\mu^2}\left[\left(\frac{1}{2}-r^2\right)\mathrm{erfc}(r) + \frac{r}{\sqrt{\pi}}e^{-r^2}\right], \end{aligned} \tag{5.28}$$

and then $w_1(y,\tau) = \tau f_1(r)$.

Results are shown in Figures 3 and 4 for $\lambda = \mu = 1$ and $n = 1$, 2, respectively. From the plot of u against x the boundary layer behavior of the right-hand edge is obvious, which confirms the analysis above.

6. Large time solution.

6.1. Linearization about the equilibrium solution. We begin the analysis by assuming that the kinetic law (2.14) is linear and thus $n = 1$. To determine the large time solution we consider a perturbation from the equilibrium solution (2.18) of the form

$$u = f(x)e^{-\gamma^2 t}, \qquad s = 1 + \frac{1}{\lambda} + S(t), \tag{6.1}$$

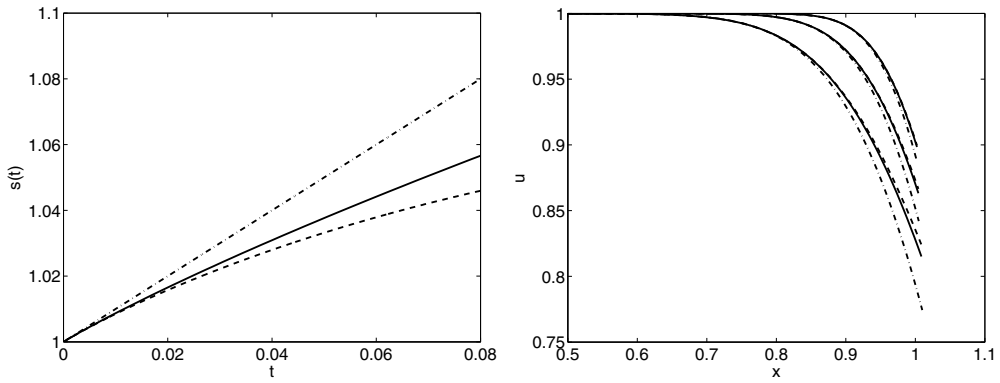

FIG. 3. *Comparison of numerical (solid line) and small time asymptotic (dot-dashed: leading-order; dashed: first-order) solutions. Left: s against t. Right: u against x (at $t = 0.0025$, 0.0049, 0.01) for $\lambda = \mu = n = 1$.*

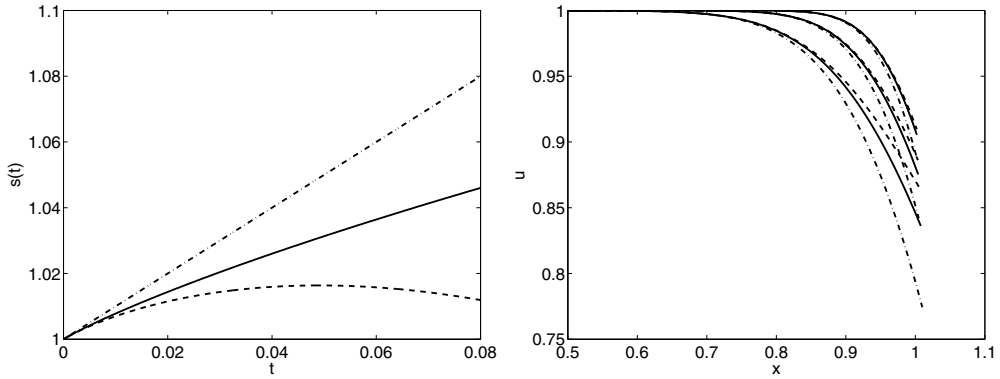

FIG. 4. *Comparison of numerical (solid line) and small time asymptotic (dot-dashed: leading-order; dashed: first-order) solutions. Left: s against t. Right: u against x (at $t = 0.0025$, 0.0049, 0.01) for $\lambda = \mu = 1$, and $n = 2$.*

where $S(t) \to 0$ as $t \to \infty$. Substituting these into the PDE (2.11), we find that f satisfies $-\gamma^2 f(x) = f''(x)$, which has general solution

$$f(x) = A\cos(\gamma x) + B\sin(\gamma x)\,. \tag{6.2}$$

The boundary condition (2.12) becomes $f'(0) = 0$, which means that $B = 0$. Combining (2.13) and (2.14) leads to the equation

$$(\lambda + u)u = -\mu\frac{\partial u}{\partial x} \qquad \text{at } x = s,$$

and so the leading-order boundary condition for f is $\lambda f(x) = -\mu f'(x)$ at $x = 1 + 1/\lambda$.

Since $f(x) = A\cos(\gamma x)$, this condition gives the following transcendental equation for γ:

$$\gamma\tan\left(\gamma\left(1 + \frac{1}{\lambda}\right)\right) = \frac{\lambda}{\mu}\,. \tag{6.3}$$

Then from (2.14) we have

$$S(t) = -\frac{A}{\mu\gamma^2}\cos\left(\gamma\left(1+\frac{1}{\lambda}\right)\right)e^{-\gamma^2 t}, \tag{6.4}$$

where the integration constant is zero to ensure that S decays as $t \to \infty$. Thus the leading-order perturbation to the equilibrium solution is

$$u = A\cos(\gamma x)\,e^{-\gamma^2 t}\,, \qquad s = 1+\frac{1}{\lambda}-\frac{A}{\mu\gamma^2}\cos\left(\gamma\left(1+\frac{1}{\lambda}\right)\right)e^{-\gamma^2 t}\,, \tag{6.5}$$

where γ satisfies (6.3). The precise value of A can be determined by patching to a numerical solution or matching to an intermediate time solution (if available).

6.2. A formal asymptotic expansion. A more formal approach would be to rescale (2.11)–(2.14) using

$$t = g(\varepsilon)+\tau\,, \qquad u(x,t) = \varepsilon v(x,\tau), \qquad s = 1+\frac{1}{\lambda}+\varepsilon S(\tau)\,, \tag{6.6}$$

where $\varepsilon \ll 1$ is an artificial parameter and $g(\varepsilon) \gg 1$, to be determined, is again the relevant time-scale over which u decays to $\mathcal{O}(\varepsilon)$. The rescaled problem is then

$$\frac{\partial v}{\partial \tau} = \frac{\partial^2 v}{\partial x^2}\,, \qquad 0 < x < 1+\frac{1}{\lambda}+\varepsilon S(\tau), \tag{6.7}$$

$$\frac{\partial v}{\partial x} = 0 \qquad \text{at } x = 0, \tag{6.8}$$

$$(\lambda+\varepsilon v)\frac{\mathrm{d}S}{\mathrm{d}\tau} = -\frac{\partial v}{\partial x} \qquad \text{at } x = 1+\frac{1}{\lambda}+\varepsilon S(\tau), \tag{6.9}$$

$$\mu\frac{\mathrm{d}S}{\mathrm{d}\tau} = v \qquad \text{at } x = 1+\frac{1}{\lambda}+\varepsilon S(\tau)\,. \tag{6.10}$$

We proceed by setting

$$S(\tau) \sim S_0(\tau)+\varepsilon S_1(\tau)+\cdots\,, \qquad v(x,\tau) \sim v_0(x,\tau)+\varepsilon v_1(x,\tau)+\cdots\,. \tag{6.11}$$

Then the leading-order problem is

$$\frac{\partial v_0}{\partial \tau} = \frac{\partial^2 v_0}{\partial x^2}\,, \qquad 0 < x < 1+\frac{1}{\lambda}, \tag{6.12}$$

$$\frac{\partial v_0}{\partial x} = 0 \qquad \text{at } x = 0, \tag{6.13}$$

$$\lambda\frac{\mathrm{d}S_0}{\mathrm{d}\tau} = -\frac{\partial v_0}{\partial x} \qquad \text{at } x = 1+\frac{1}{\lambda}, \tag{6.14}$$

$$\mu\frac{\mathrm{d}S_0}{\mathrm{d}\tau} = v_0 \qquad \text{at } x = 1+\frac{1}{\lambda}\,. \tag{6.15}$$

As before, we try a solution for v_0 of the form $v_0(x,\tau) = f_0(x)e^{-\gamma_0^2\tau}$. The leading-order solution turns out to be identical to that given in section 6.1 but in the rescaled variables, namely,

$$v_0(x,\tau) = A_0\cos(\gamma_0 x)\,e^{-\gamma_0^2\tau}\,, \qquad S_0(\tau) = D_0 e^{-\gamma_0^2\tau}\,, \tag{6.16}$$

where $D_0 = -A_0\cos(\gamma_0(1+1/\lambda))/[\mu\gamma_0^2]$ and γ_0 satisfies (6.3). The value of A_0 can again be found by patching.

To determine $g(\varepsilon)$ we revert to original variables and write

$$u(x,t) = \varepsilon A_0 \cos(\gamma_0 x)\, e^{-\gamma_0^2(t-g(\varepsilon))}\,, \qquad s = 1 + \frac{1}{\lambda} + \varepsilon D_0 e^{-\gamma_0^2(t-g(\varepsilon))}\,. \tag{6.17}$$

We must choose $g(\varepsilon)$ to eliminate the artificial parameter; i.e., $\varepsilon e^{\gamma_0^2 g(\varepsilon)} = 1$ or

$$\gamma_0^2 g(\varepsilon) = \ln(1/\varepsilon) \qquad \Longrightarrow \qquad g(\varepsilon) = \frac{\ln(1/\varepsilon)}{\gamma_0^2}\,. \tag{6.18}$$

Then the solutions in (6.17) reduce to

$$u(x,t) = A_0 \cos(\gamma_0 x)\, e^{-\gamma_0^2 t}\,, \qquad s = 1 + \frac{1}{\lambda} + D_0 e^{-\gamma_0^2 t}\,. \tag{6.19}$$

Note that this is precisely the same form as the HBIM large time asymptotic solution given in (4.9), and so we can compare γ_0^2 with k/μ. With $\mu = \lambda = 1$ and $m \approx 2.5836$ we find that $\gamma_0 \approx 0.540$ and $\sqrt{k/\mu} \approx 0.529$, which shows an excellent agreement.

The $\mathcal{O}(\varepsilon)$ problem is

$$\frac{\partial v_1}{\partial \tau} = \frac{\partial^2 v_1}{\partial x^2}\,, \qquad 0 < x < 1 + \frac{1}{\lambda}, \tag{6.20}$$

$$\frac{\partial v_1}{\partial x} = 0 \qquad \text{at } x = 0, \tag{6.21}$$

$$\lambda \frac{\mathrm{d}S_1}{\mathrm{d}\tau} + v_0 \frac{\mathrm{d}S_0}{\mathrm{d}\tau} + \frac{\partial^2 v_0}{\partial x^2} S_0 = -\frac{\partial v_1}{\partial x} \qquad \text{at } x = 1 + \frac{1}{\lambda}, \tag{6.22}$$

$$\mu \frac{\mathrm{d}S_1}{\mathrm{d}\tau} = \frac{\partial v_0}{\partial x} S_0 + v_1 \qquad \text{at } x = 1 + \frac{1}{\lambda}\,, \tag{6.23}$$

where we have expanded the boundary conditions at the moving front using a Taylor series about $1 + 1/\lambda$. Here we seek a solution of the form $v_1(x,\tau) = f_1(x)e^{-\gamma_1^2\tau}$. It again follows from (6.20) and (6.21) that $f_1(x) = A_1 \cos(\gamma_1 x)\, e^{-\gamma_1^2\tau}$, and the free boundary conditions (6.22) and (6.23) give $\gamma_1^2 = 2\gamma_0^2$. This is to be expected since the leading- and first-order solutions, namely v_0 and v_1, respectively, are the first two terms in an infinite series solution for v. Then we can write $S_1(\tau) = D_1 e^{-2\gamma_0^2\tau}$. The coefficients A_1 and D_1 are found from (6.22) and (6.23), and these are defined in terms of A_0, D_0, γ_0, and γ_1. After some manipulation we find

$$A_1 = -\frac{A_0 D_0 \gamma_0 \big[2\mu\gamma_0 \cos(\gamma_0(1+\frac{1}{\lambda})) + \lambda \sin(\gamma_0(1+\frac{1}{\lambda}))\big]}{-\lambda \cos(\gamma_1(1+\frac{1}{\lambda})) + \mu\gamma_1(\gamma_1(1+\frac{1}{\lambda}))},$$

$$D_1 = \frac{A_0 D_0 \gamma_0 \big[2\gamma_0 \cos(\gamma_0(1+\frac{1}{\lambda}))\cos(\gamma_1(1+\frac{1}{\lambda})) + \gamma_1 \sin(\gamma_1(1+\frac{1}{\lambda}))\sin(\gamma_0(1+\frac{1}{\lambda}))\big]}{\gamma_1^2\big[-\lambda\cos(\gamma_1(1+\frac{1}{\lambda})) + \mu\gamma_1(\gamma_1(1+\frac{1}{\lambda}))\big]}\,.$$

Figure 5 gives results for $n = 1$. The patching has been carried out at time $t = 4$. Observe that, even for this relatively small time, the asymptotic solutions closely match the numerical solutions. However, for u we need to consider larger values of t to obtain a similar level of accuracy, but even for $t = 9$ the approximation is good. Note that as λ is increased, we can choose even smaller times to give a solution with the same level of accuracy. Indeed, for $\lambda = 2$ the plots analogous to those in Figure 5 are virtually indistinguishable from the numerical solution.

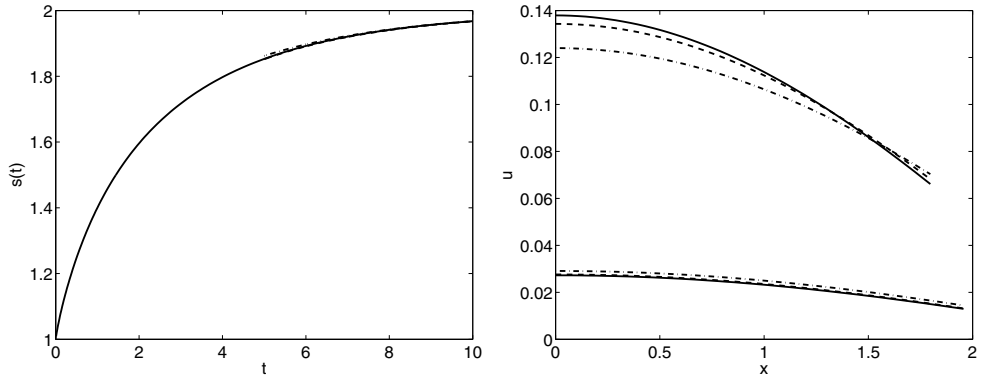

FIG. 5. *Comparison of numerical (solid line) and large time asymptotic (dot-dashed: leading-order; dashed: first-order) solutions. Left: s against t. Right: u against x (at $t = 4, 9$) for $\lambda = \mu = n = 1$.*

This formal approach allows us to consider the case when $n > 1$. Following the large time approximation to the HBIM solution in section 4, we use a similar scaling to (4.4) and set

$$t = g(\varepsilon) + \varepsilon^{1-n}\tau\,, \qquad u(x,t) = \varepsilon v(x,\tau)\,, \qquad s = 1 + \frac{1}{\lambda} + \varepsilon S(\tau)\,. \tag{6.24}$$

The rescaled problem is now

$$\varepsilon^{n-1}\frac{\partial v}{\partial \tau} = \frac{\partial^2 v}{\partial x^2}\,, \qquad 0 < x < 1 + \frac{1}{\lambda} + \varepsilon S(\tau), \tag{6.25}$$

$$\frac{\partial v}{\partial x} = 0 \qquad \text{at } x = 0, \tag{6.26}$$

$$(\lambda + \varepsilon v)\varepsilon^{n-1}\frac{\mathrm{d}S}{\mathrm{d}\tau} = -\frac{\partial v}{\partial x} \qquad \text{at } x = 1 + \frac{1}{\lambda} + \varepsilon S(\tau), \tag{6.27}$$

$$\mu\frac{\mathrm{d}S}{\mathrm{d}\tau} = v^n \qquad \text{at } x = 1 + \frac{1}{\lambda} + \varepsilon S(\tau)\,. \tag{6.28}$$

A natural starting point is to consider $n = 2$, since then $\mathcal{O}(\varepsilon)$ terms appear in (6.25) and (6.27). Using the expansions in (6.11), we find that the leading-order problem reduces to

$$\frac{\partial^2 v_0}{\partial x^2} = 0\,, \qquad 0 < x\frac{1}{\lambda}la, \tag{6.29}$$

$$\frac{\partial v_0}{\partial x} = 0 \qquad \text{at } x = 0, \tag{6.30}$$

$$\frac{\partial v_0}{\partial x} = 0 \qquad \text{at } x = 1 + \frac{1}{\lambda}, \tag{6.31}$$

$$\mu\frac{\mathrm{d}S_0}{\mathrm{d}\tau} = {v_0}^2 \qquad \text{at } x = 1 + \frac{1}{\lambda}\ . \tag{6.32}$$

Solving (6.29)–(6.31), we find that v_0 is simply a constant in x, i.e., $v_0 = B_0(\tau)$, and (6.31) is

$$\mu\frac{\mathrm{d}S_0}{\mathrm{d}\tau} = {B_0}^2\,. \tag{6.33}$$

To determine B_0 we need to go to the next order. The $\mathcal{O}(\varepsilon)$ equations are

$$\frac{\partial v_0}{\partial \tau} = \frac{\partial^2 v_1}{\partial x^2}\,, \qquad 0 < x < 1 + \frac{1}{\lambda}, \tag{6.34}$$

$$\frac{\partial v_1}{\partial x} = 0 \qquad \text{at } x = 0, \tag{6.35}$$

$$\lambda \frac{\mathrm{d}S_0}{\mathrm{d}\tau} = -\frac{\partial^2 v_0}{\partial x^2} S_0 - \frac{\partial v_1}{\partial x} \qquad \text{at } x = 1 + \frac{1}{\lambda}, \tag{6.36}$$

$$\mu \frac{\mathrm{d}S_1}{\mathrm{d}\tau} = 2v_0 \left(\frac{\partial v_0}{\partial x} S_0 + v_1 \right) \qquad \text{at } x = 1 + \frac{1}{\lambda}\,, \tag{6.37}$$

where we have again expanded the boundary conditions at the moving front using a Taylor series about $1 + 1/\lambda$. Solving (6.34) and (6.35), we obtain

$$v_1 = \frac{1}{2} B_0'(\tau) x^2 + B_1(\tau)\,, \tag{6.38}$$

and substituting this expression into (6.36) then leads to

$$\lambda \frac{\mathrm{d}S_0}{\mathrm{d}\tau} = -B_0'(\tau) \left(1 + \frac{1}{\lambda} \right). \tag{6.39}$$

Combining this with (6.33) then leads to an ODE for B_0, which can be solved to give

$$B_0(\tau) = \frac{\mu(1+\lambda)}{C + \lambda^2 \tau}\,. \tag{6.40}$$

Finally, we substitute this into (6.33) to determine S_0, i.e.,

$$S_0(\tau) = -\frac{\mu(1+\lambda)^2}{\lambda^2 (C + \lambda^2 \tau)}\,, \tag{6.41}$$

where the integration constant is set to zero to ensure that S_0 decays to zero. Translating these solutions back into the original variables, we have

$$u = \frac{\mu(1+\lambda)}{F + \lambda^2 t}\,, \qquad s = 1 + \frac{1}{\lambda} - \frac{\mu(1+\lambda)^2}{\lambda^2 [F + \lambda^2 t]}\,, \tag{6.42}$$

with $g(\varepsilon)$ chosen so that $F = \varepsilon^{-1} C - \lambda^2 g(\varepsilon)$.

Figure 6 shows results for $n = 2$. The patching is again carried out at $t = 4$. This can be compared directly with Figure 5 since the only difference is the value of n. In the plots for u we have also included $t = 25$, as the results for $t = 4$, 9 are quite inaccurate. This is not surprising since the leading-order expression for u in (6.42) is independent of x.

It can be shown that the same analysis holds for all $n > 1$. Due to the $\mathcal{O}(\varepsilon^{n-1})$ terms appearing in (6.25) and (6.27), the expansions change depending on whether $n \leq 2$ or $n > 2$. Hence we set

$$S(\tau) \sim S_0(\tau) + \varepsilon^{n-1} S_1(\tau) + \cdots\,,$$
$$v(x,\tau) \sim v_0(x,\tau) + \varepsilon^{n-1} v_1(x,\tau) + \cdots$$

for $1 < n \leq 2$, and

$$S(\tau) \sim S_0(\tau) + \varepsilon S_1(\tau) + \varepsilon^{n-1} S_2(\tau) + \cdots\,,$$
$$v(x,\tau) \sim v_0(x,\tau) + \varepsilon v_1(x,\tau) + \varepsilon^{n-1} v_2(x,\tau) + \cdots$$

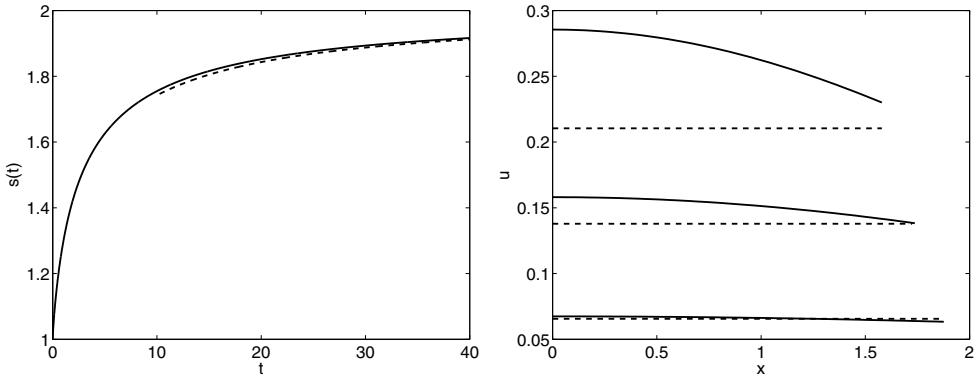

FIG. 6. *Comparison of numerical (solid line) and leading-order large time asymptotic (dashed line) solutions. Left: s against t. Right: u against x (at $t = 4, 9, 25$) for $\lambda = \mu = 1$, $n = 2$.*

for $n > 2$. In both cases, the $\mathcal{O}(\varepsilon^0)$ and $\mathcal{O}(\varepsilon^{n-1})$ terms lead to the ODEs

$$\mu \frac{\mathrm{d}S_0}{\mathrm{d}\tau} = {B_0}^n, \qquad \lambda \frac{\mathrm{d}S_0}{\mathrm{d}\tau} = -B_0'(\tau)\left(1 + \frac{1}{\lambda}\right), \tag{6.43}$$

which have solutions

$$B_0(\tau) = \left(\frac{\mu(1+\lambda)}{C + (n-1)\lambda^2\tau}\right)^{\frac{1}{n-1}} \tag{6.44}$$

and

$$S_0(\tau) = -\frac{1}{\lambda^2}\left(\frac{\mu(1+\lambda)^n}{C + (n-1)\lambda^2\tau}\right)^{\frac{1}{n-1}}. \tag{6.45}$$

Translating these solutions back into the original variables gives

$$u = \left(\frac{\mu(1+\lambda)}{F + (n-1)\lambda^2 t}\right)^{\frac{1}{n-1}}, \qquad s = 1 + \frac{1}{\lambda} - \frac{1}{\lambda^2}\left(\frac{\mu(1+\lambda)^n}{F + (n-1)\lambda^2 t}\right)^{\frac{1}{n-1}}, \tag{6.46}$$

with $g(\varepsilon)$ again chosen so that $F = \varepsilon^{1-n}C - (n-1)\lambda^2 g(\varepsilon)$ and the expression for s precisely agrees with that in (4.12).

The results are presented in Figure 7 for $n = 3$ with patching carried out at $t = 9$. Observe that even larger values of t are required for the asymptotic expansion to give good agreement, which is to be expected since the time-scale $t \sim \varepsilon^{1-n}\tau$. It is clear that as n increases, the range of validity of the large time solution decreases. It is worth highlighting here that the solution structure is very different for $n = 1$ and $n > 1$, with u being independent of x in the latter case in contrast to the former, which is given in (6.19). This shows how important it is to consider in detail the nonlinear case, as discussed in the introduction.

7. Large parameter expansions. In the small- and large time expansions considered in sections 5 and 6, we assumed that $\lambda = \mu = \mathcal{O}(1)$. However, a physically relevant situation arises when $\lambda \gg 1$ and $\mu = \mathcal{O}(1)$, as discussed in [14, 17]. Another case of interest is to consider λ, $\mu \gg 1$, which occurs when $u_i - u^*$ is small, as discussed in section 2.

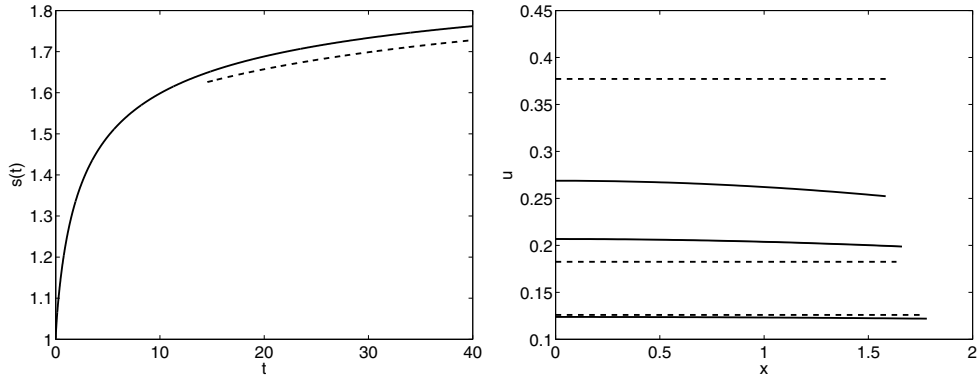

FIG. 7. *Comparison of numerical (solid line) and large time asymptotic (dashed line) solutions. Left: s against t for $\lambda = \mu = 1$ and $n = 3$. Right: u against x (at $t = 9$, 16, 49) for $\lambda = \mu = 1$, $n = 3$.*

7.1. $\lambda \gg 1$, $\mu = \mathcal{O}(1)$. If we set $\varepsilon = 1/\lambda \ll 1$, noting that ε is a real (as distinct from artificial) parameter, then (2.11)–(2.15) become

$$\frac{\partial u}{\partial t} = \frac{\partial^2 u}{\partial x^2}, \qquad 0 < x < s, \tag{7.1}$$

$$\frac{\partial u}{\partial x} = 0 \qquad \text{at } x = 0, \tag{7.2}$$

$$(1 + \varepsilon u)\frac{\mathrm{d}s}{\mathrm{d}t} = -\varepsilon \frac{\partial u}{\partial x} \qquad \text{at } x = s, \tag{7.3}$$

$$\mu \frac{\mathrm{d}s}{\mathrm{d}t} = u^n \qquad \text{at } x = s, \tag{7.4}$$

$$s = 1 \text{ and } u = 1 \qquad \text{at } t = 0. \tag{7.5}$$

Time is rescaled by setting $t = \tau/\varepsilon$. Then the leading-order terms satisfy

$$\frac{\partial^2 u}{\partial x^2} = 0, \qquad 0 < x < s, \tag{7.6}$$

$$\frac{\partial u}{\partial x} = 0 \qquad \text{at } x = 0, \tag{7.7}$$

$$\frac{\mathrm{d}s}{\mathrm{d}\tau} = -\frac{\partial u}{\partial x} \qquad \text{at } x = s, \tag{7.8}$$

$$u = 0 \qquad \text{at } x = s, \tag{7.9}$$

$$s = 1 \text{ and } u = 1 \qquad \text{at } \tau = 0, \tag{7.10}$$

and we just recover the steady state which has outer solution $u = 0$ and $s = 1$. Now, the solution for u does not satisfy the initial condition, and so we return to the original equations (7.1)–(7.5). The boundary condition (7.3) and initial condition (7.5) immediately give $s = 1$, as expected from the rescaled equations. Thus we consider an expansion of the form

$$u = u_0 + \varepsilon u_1 + \cdots, \qquad s = 1 + \varepsilon s_0 + \cdots. \tag{7.11}$$

The leading-order equations then reduce to

$$\frac{\partial u_0}{\partial t} = \frac{\partial^2 u_0}{\partial x^2}, \qquad 0 < x < 1, \tag{7.12}$$

$$\frac{\partial u_0}{\partial x} = 0 \qquad \text{at } x = 0, \tag{7.13}$$

$$u_0 = 0 \qquad \text{at } x = 1, \tag{7.14}$$

$$u_0 = 1 \qquad \text{at } t = 0\,. \tag{7.15}$$

The solution can be found using Fourier series. Thus

$$u_0(x,t) = \sum_{k=1}^{\infty} A_k \cos(\gamma_k x) \exp(-\gamma_k^2 t)\,, \tag{7.16}$$

where

$$A_k = \frac{2\sin\gamma_k}{\gamma_k} \tag{7.17}$$

and $\gamma_k = (k - 1/2)\pi$. To determine s_0 we turn to the $\mathcal{O}(\varepsilon)$ equations. At this order the boundary condition (7.3) becomes

$$\frac{\mathrm{d}s_0}{\mathrm{d}t} = -\frac{\partial u_0}{\partial x} \qquad \text{at } x = 1\,. \tag{7.18}$$

A straightforward calculation gives

$$s_0 = \sum_{k=1}^{\infty} \frac{2\sin^2\gamma_k}{\gamma_k^2}\left[1 - \exp(-\gamma_k^2 t)\right], \tag{7.19}$$

and so $s = 1 + s_0/\lambda$ up to first order. It should be noted that this solution is, in fact, valid only for $n = 1$. For $n > 1$, the $\mathcal{O}(\varepsilon)$ equations for the boundary condition (7.4) lead to

$$\mu\frac{\mathrm{d}s_0}{\mathrm{d}t} = u_0^{n-1} n \left(\frac{\partial u_0}{\partial x} s_0 + u_1\right) \qquad \text{at } x = 1\,, \tag{7.20}$$

and then, using (7.14), this shows that $\frac{\mathrm{d}s_0}{\mathrm{d}t} = 0$, which contradicts (7.19). For $n = 2$, the rescaling $u = \varepsilon v$, $s \sim 1 + \varepsilon + \varepsilon^2 S(\tau)$, $t = \tau/\varepsilon$ leads to a consistent problem with a nonlinear boundary condition, but this cannot be solved analytically.

Even for $n = 1$ there is no closed form solution for u_1, since the boundary condition (7.20) involves an infinite series expansion. Hence we show results only for $u = u_0$, $s = 1 + s_0/\lambda$, which are given in Figure 8. The left-hand plots of s against t show that the asymptotic solution becomes more accurate as λ increases, as expected. The same is true in the right-hand plots, which show u against x at a fixed $t = 1$. Since the leading-order solution for u does not contain λ, we have included three plots of the numerical solution for different values of λ. It is clear that as λ increases, the leading-order asymptotic solution becomes more accurate.

Note that an alternative series solution to (7.12)–(7.15) can be found using Laplace transforms. This is given by

$$u_0(x,t) = 1 - \sum_{k=0}^{\infty}(-1)^k \operatorname{erfc}\left(\frac{1+2k+x}{2\sqrt{t}}\right) - \sum_{k=0}^{\infty}(-1)^k \operatorname{erfc}\left(\frac{1+2k-x}{2\sqrt{t}}\right), \tag{7.21}$$

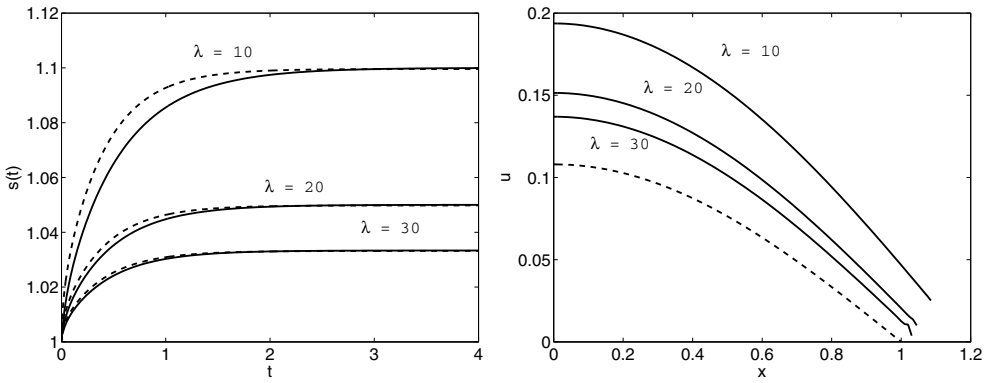

FIG. 8. *Comparison of numerical (solid line) and $\lambda \gg 1$, $\mu = \mathcal{O}(1)$ asymptotic (dashed line) solutions. Left: s against t (for $\lambda = 10, 20, 30$, $\mu = n = 1$). Right: u against x (at $t = 1$).*

and then, using (7.18), we have

$$s_0 = 2\sqrt{\frac{t}{\pi}} + 4\sum_{k=1}^{\infty}(-1)^k \left[\sqrt{\frac{t}{\pi}}\exp\left(-\frac{k^2}{t}\right) - k\,\mathrm{erfc}\left(\frac{k}{\sqrt{t}}\right)\right], \tag{7.22}$$

leading to $s = 1 + s_0/\lambda$. This form of the solution gives results identical to those from the Fourier series solution and is useful when comparisons are made with the small time solution below.

7.1.1. Comparison with the small time solution, $\boldsymbol{\lambda \gg 1}$, $\boldsymbol{\mu = \mathcal{O}(1)}$. It is not possible to directly compare the large λ results given above for small times with the results in section 5 for large λ. This is clear from examining (5.4), which needs rescaling when $\lambda \gg 1$. It is simpler to use $\varepsilon \equiv 1/\lambda \ll 1$ as a small parameter and rescale (2.11)–(2.15) directly; we can find a closed form solution via $t = \varepsilon\tau$, which gives

$$\frac{\partial u}{\partial \tau} = \varepsilon\frac{\partial^2 u}{\partial x^2}, \qquad 0 < x < s, \tag{7.23}$$

$$\frac{\partial u}{\partial x} = 0 \qquad \text{at } x = 0, \tag{7.24}$$

$$(1+\varepsilon u)\frac{\mathrm{d}s}{\mathrm{d}\tau} = -\varepsilon^2\frac{\partial u}{\partial x} \qquad \text{at } x = s, \tag{7.25}$$

$$\mu\frac{\mathrm{d}s}{\mathrm{d}\tau} = \varepsilon u^n \qquad \text{at } x = s, \tag{7.26}$$

$$s = 1 \text{ and } u = 1 \qquad \text{at } \tau = 0. \tag{7.27}$$

The leading-order terms satisfy $u_\tau = 0$, $u_x = 0$ at $x = 0$, and so, combining this with the initial conditions in (7.27), it follows that the outer solution is $u \sim 1$, $s \sim 1$. However, that will not satisfy the boundary conditions at the right edge, and so a boundary layer must exist, similar to that discussed in section 5. To incorporate this we rescale by setting

$$s(\tau) \sim 1 + \varepsilon^{3/2}L(\tau)\,, \qquad x = 1 + \varepsilon^{3/2}L(\tau) - \sqrt{\varepsilon}y\,, \qquad u(x,\tau) = v(y,\tau)\,. \tag{7.28}$$

Then the system becomes

$$\frac{\partial v}{\partial \tau} + \varepsilon \frac{\mathrm{d}L}{\mathrm{d}\tau}\frac{\partial v}{\partial y} = \frac{\partial^2 v}{\partial y^2}, \qquad 0 < y < \infty, \tag{7.29}$$

$$(1+\varepsilon v)\frac{\mathrm{d}L}{\mathrm{d}\tau} = \frac{\partial v}{\partial y} \qquad \text{at } y = 0, \tag{7.30}$$

$$\mu\sqrt{\varepsilon}\frac{\mathrm{d}L}{\mathrm{d}\tau} = v^n \qquad \text{at } y = 0, \tag{7.31}$$

$$v \to 1 \qquad \text{as } y \to \infty, \tag{7.32}$$

where the condition (7.32) comes from matching the $x = 0$ boundary (now transformed to $y \to \infty$) with the outer solution $u = 1$.

The leading-order terms in (7.29), (7.31), and (7.32) give rise to the classical error function solution,

$$v_0 = 1 - \operatorname{erfc}\left(\frac{y}{2\sqrt{\tau}}\right), \tag{7.33}$$

and then (7.30) shows that $L_0 = 2\sqrt{\tau/\pi}$. The solutions in the original variables are therefore

$$u_0 = 1 - \operatorname{erfc}\left(\frac{s-x}{2\sqrt{t}}\right), \qquad s = 1 + \frac{2}{\lambda}\sqrt{\frac{t}{\pi}}. \tag{7.34}$$

The aim is now to compare these solutions with those determined in section 7.1. However, let us consider (7.16) and attempt to expand the exponential term for small t in powers of t. Specifically, the expansion of (7.16) would lead to a Taylor series of the form

$$\begin{aligned} u(x,t) &\sim u(x,0) + t\frac{\partial u}{\partial t}(x,0) + \frac{t^2}{2!}\frac{\partial^2 u}{\partial t^2}(x,0) + \cdots \\ &= u(x,0) + t\frac{\partial^2 u}{\partial x^2}(x,0) + \frac{t^2}{2!}\frac{\partial^4 u}{\partial x^4}(x,0) + \cdots, \end{aligned}$$

using the fact that $u_t = u_{xx}$. Due to the nature of the boundary condition at $x = 1$, $u(x,0)$ is a discontinuous step function, and so its Fourier series may not be differentiated. However, we can simply plot (7.16) and (7.19) (which is valid for all t), and we show this comparison in Figure 9 for small times.

The solutions (7.21) and (7.22), found using Laplace transforms, are more convenient for this comparison. Using the fact that

$$\operatorname{erfc}(z) \sim e^{-z}\left[\frac{1}{\sqrt{\pi}z} - \frac{1}{2\sqrt{\pi}z^3} + \cdots\right]$$

for $z \gg 1$, it follows that the summation term in (7.22) is $\mathcal{O}(t^{3/2}e^{-k^2/t}/k^2)$, and so for small times s matches that given in (7.34). On examining (7.21), we find for $t \ll 1$ that

$$u_0 \sim 1 - \operatorname{erfc}\left(\frac{1-x}{2\sqrt{t}}\right),$$

which agrees with that given in (7.34) at leading order.

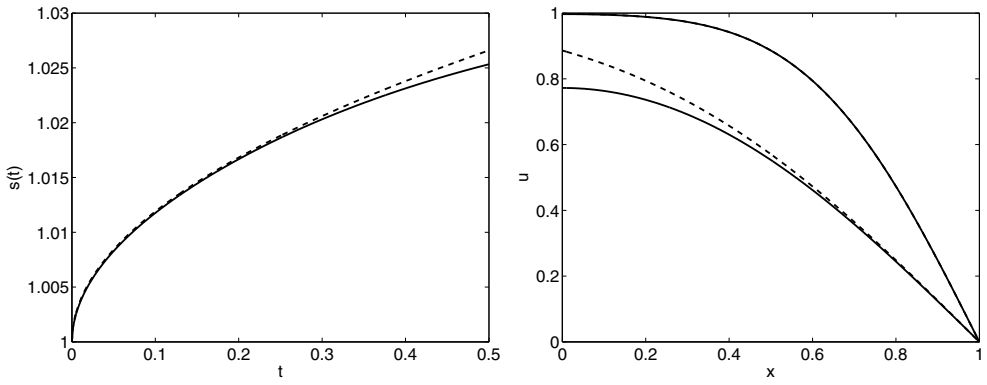

FIG. 9. *Comparison of* (7.16), (7.19) *(solid line) with* (7.34) *(dashed line) for small times and* $\lambda \gg 1$, $\mu = \mathcal{O}(1)$. *Left: s against t (for* $\lambda = 30$, $\mu = n = 1$*). Right: u against x (at* $t = 0.05$ *and* $t = 0.2$*).*

7.1.2. Comparison with the large time solution, $\lambda \gg 1$, $\mu = \mathcal{O}(1)$. In this case we can make direct comparisons with the solutions in sections 6 and 7.1 when considering large λ and large time limits, respectively.

If we set $\lambda \equiv 1/\varepsilon$ in (6.3) and expand for $\varepsilon \ll 1$, then we find that

$$\gamma \sim \frac{\pi}{2} - \frac{\pi}{2}(1+\mu)\varepsilon + \cdots . \tag{7.35}$$

Thus, the solutions in (6.19) at leading order become

$$u = A\cos\left(\frac{\pi x}{2}\right) e^{-\pi^2 t/4}, \qquad s = 1. \tag{7.36}$$

Now, the first term in the series solution (7.16) is simply

$$u_0 = A_1 \cos(\gamma_1 x) e^{-\gamma_1^2 t} = \frac{4}{\pi}\cos\left(\frac{\pi x}{2}\right) e^{-\pi^2 t/4}, \tag{7.37}$$

which agrees with (7.36) and actually ties down the coefficient A in this limit. Also, (7.19) comes in at $\mathcal{O}(\varepsilon)$, and so at leading order $s = 1$, which also agrees with that given in (7.36).

7.2. λ, $\mu \gg 1$. Although a two parameter expansion is possible, let us choose a distinguished limit by setting $\mu = a\lambda$, where $a = \mathcal{O}(1)$. Then with $\varepsilon = 1/\lambda \ll 1$ we also obtain (7.1)–(7.5), except that (7.4) is replaced by

$$a\frac{\mathrm{d}s}{\mathrm{d}t} = \varepsilon u^n \qquad \text{at } x = s. \tag{7.38}$$

After rescaling time by setting $t = \tau/\varepsilon$, we again recover the steady-state solution $u = 0$, $s = 1$. Hence we return to the original equations and have

$$\frac{\partial u}{\partial t} = \frac{\partial^2 u}{\partial x^2}\,, \qquad 0 < x < s, \tag{7.39}$$

$$\frac{\partial u}{\partial x} = 0 \qquad \text{at } x = 0, \tag{7.40}$$

$$(1 + \varepsilon u)u^n = -a\frac{\partial u}{\partial x} \qquad \text{at } x = s, \tag{7.41}$$

$$a\frac{\mathrm{d}s}{\mathrm{d}t} = \varepsilon u^n \qquad \text{at } x = s, \tag{7.42}$$

$$s = 1 \text{ and } u = 1 \qquad \text{at } t = 0. \tag{7.43}$$

Note that (7.41) comes from combining (7.3) and (7.38) and dividing through by ε. With the same expansions for u and s as in (7.11), we find that the leading-order equations now reduce to

$$\frac{\partial u_0}{\partial t} = \frac{\partial^2 u_0}{\partial x^2}\,, \qquad 0 < x < 1, \tag{7.44}$$

$$\frac{\partial u_0}{\partial x} = 0 \qquad \text{at } x = 0, \tag{7.45}$$

$${u_0}^n = -a\frac{\partial u_0}{\partial x} \qquad \text{at } x = 1, \tag{7.46}$$

$$u_0 = 1 \qquad \text{at } t = 0. \tag{7.47}$$

Provided $n = 1$, the solution can now be determined using Fourier series. In the nonlinear case we would have to solve (7.44)–(7.47) numerically. For simplicity we set $a = 1$ and consider the linear case $n = 1$. The solution is again given by (7.16), but now the A_k's satisfy

$$A_k = \frac{2\sin\gamma_k}{\gamma_k + \cos\gamma_k \sin\gamma_k}\,, \tag{7.48}$$

and the γ_k's satisfy the transcendental equation

$$1 = \gamma_k \tan\gamma_k\,. \tag{7.49}$$

In this case the condition (7.42) at $\mathcal{O}(\varepsilon)$ gives s_0, and we find that

$$s_0 = \sum_{k=1}^{\infty} \frac{A_k \cos\gamma_k}{\gamma_k^2}\left[1 - \exp(-\gamma_k^2 t)\right], \tag{7.50}$$

and again $s = 1 + s_0/\lambda$ at leading order. For the $\mathcal{O}(\varepsilon)$ equations, u_1 satisfies (7.44), (7.45), and (7.47), and (7.41) becomes

$$u_1 + u_0^2 + \frac{\partial u_0}{\partial x}s_0 = -a\left(\frac{\partial^2 u_0}{\partial x^2}s_0 + \frac{\partial u_1}{\partial x}\right) \qquad \text{at } x = 1. \tag{7.51}$$

This also does not have a closed form solution, and so we give only leading-order results for u, as before. Note that Cohen and Erneux [5] also obtained these results in their limit of interest, with allowances made for the different scalings. The leading-order solutions are shown in Figure 10. The left-hand plots of s against t show that

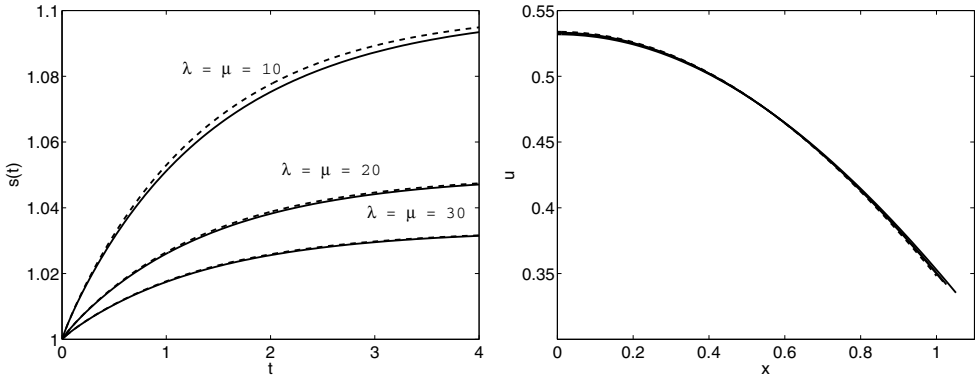

FIG. 10. *Comparison of numerical (solid line) and* $\lambda = \mu \gg 1$ *asymptotic (dashed line) solutions. Left:* s *against* t *(for* $\lambda = \mu = 10$, 20, 30, $n = 1$*). Right:* u *against* x *(at* $t = 1$*).*

the asymptotic solution becomes more accurate as λ increases, as expected, and the convergence is quicker than when $\lambda \gg 1$ and $\mu = \mathcal{O}(1)$ (comparing the left-hand plots of Figures 8 and 10). It is interesting to note that in the right-hand plot, which shows u against x at a fixed $t = 1$, it is hard to distinguish the three numerical solutions (at $\lambda = \mu = 10$, 20, 30) from the leading-order asymptotic solution. This is significantly different from the plots for u shown in Figure 8.

7.2.1. Comparison with the small time solution, $\lambda, \mu \gg 1$. Here we follow the analysis described in section 7.1.1 and set $\lambda = 1/\varepsilon$, $t = \varepsilon\tau$ with $\mu = a/\varepsilon$. Equations (7.23)–(7.25), (7.27) are unchanged, and (7.26) becomes

$$a\frac{\mathrm{d}s}{\mathrm{d}\tau} = \varepsilon^2 u^n \qquad \text{at } x = s. \tag{7.52}$$

The outer solution is again $u \sim 1$, $s \sim 1$, and a boundary layer also exists at the right edge. To incorporate this we rescale by setting

$$s(\tau) \sim 1 + \varepsilon^2 L(\tau)\,, \quad x = 1 + \varepsilon^2 L(\tau) - \sqrt{\varepsilon} y\,, \quad u(x,\tau) = 1 + \sqrt{\varepsilon} v(y,\tau)\,. \tag{7.53}$$

Then the system becomes

$$\frac{\partial v}{\partial \tau} + \varepsilon^{3/2}\frac{\mathrm{d}L}{\mathrm{d}\tau}\frac{\partial v}{\partial y} = \frac{\partial^2 v}{\partial y^2}, \qquad 0 < y < \infty, \tag{7.54}$$

$$(1 + \varepsilon + \varepsilon^{3/2} v)\frac{\mathrm{d}L}{\mathrm{d}\tau} = \frac{\partial v}{\partial y} \qquad \text{at } y = 0, \tag{7.55}$$

$$a\frac{\mathrm{d}L}{\mathrm{d}\tau} = (1 + \sqrt{\varepsilon} v)^n \qquad \text{at } y = 0, \tag{7.56}$$

$$v \to 0 \qquad \text{as } y \to \infty. \tag{7.57}$$

The leading-order terms (after combining (7.55) and (7.56)) give the solution

$$v_0 = -\frac{1}{a}\left[2\sqrt{\frac{\tau}{\pi}}\exp\left(-\frac{y^2}{4\tau}\right) - y\,\mathrm{erfc}\left(\frac{y}{2\sqrt{\tau}}\right)\right], \tag{7.58}$$

and then (7.56) shows that $L_0 = \tau/a$. The solutions in the original variables are

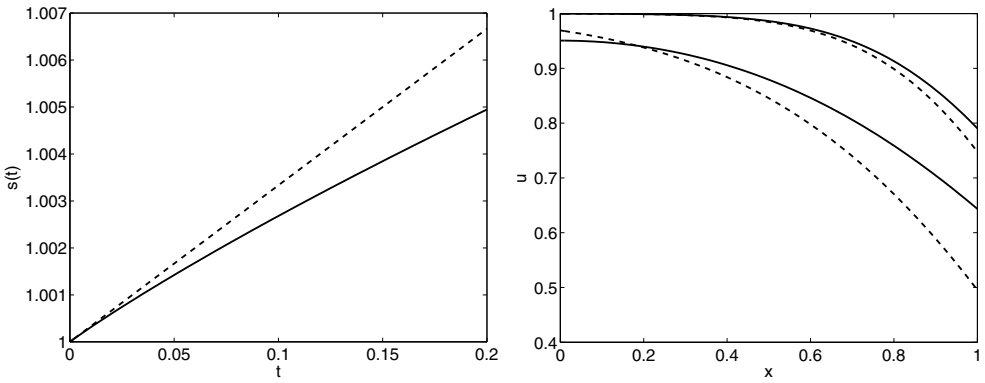

FIG. 11. *Comparison of* (7.16), (7.50) *(solid line) with* (7.59) *(dashed line) for small times and* λ, $\mu \gg 1$. *Left:* s *against* t *(for* $\lambda = \mu = 30$, $n = 1$*). Right:* u *against* x *(at* $t = 0.05$ *and* $t = 0.2$*).*

therefore

(7.59)
$$u_0 = 1 - \frac{1}{a}\left[2\sqrt{\frac{t}{\pi}}\exp\left(-\frac{(s-x)^2}{4t}\right) - (s-x)\operatorname{erfc}\left(\frac{s-x}{2\sqrt{t}}\right)\right], \qquad s = 1 + \frac{t}{\lambda a}.$$

As before, it is not possible to expand the Fourier series solution from section 7.2 directly for small t. However, in Figure 11 we simply directly compare (7.59) and the Fourier series solution for large λ, μ.

7.2.2. Comparison with the large time solution, λ, $\mu \gg 1$. Here we set $\lambda = 1/\varepsilon$, $\mu = a\lambda = a/\varepsilon$ in (6.3) and expand for $\varepsilon \ll 1$. For comparison purposes and without loss of generality, we take $a = 1$. We find that γ satisfies the transcendental equation

$$\gamma \tan\gamma = 1 \tag{7.60}$$

at leading order. Thus, the solutions (6.19) at leading order become

$$u = A\cos(\gamma x)e^{-\gamma^2 t}, \qquad s = 1. \tag{7.61}$$

Now, the first term in the series solution (7.16) is simply

$$u_0 = A_1\cos(\gamma_1 x)e^{-\gamma_1^2 t}, \tag{7.62}$$

where γ_1 satisfies $\gamma_1 \tan\gamma_1 = 1$, which agrees with (7.61). Again, since (7.49) comes in at $\mathcal{O}(\varepsilon)$, the leading-order solution is simply $s = 1$, which also agrees with that given in (7.61).

8. Conclusions. In this paper we have considered numerical, approximate, and asymptotic approximate techniques applied to a one-dimensional moving boundary problem describing the diffusion within glassy polymers. We have highlighted an accurate numerical scheme, which immobilizes the boundary to give a fixed domain and uses a similarity transformation to ensure the correct asymptotic structure in the limit as $t \to 0^+$. The heat balance integral method was applied to the problem, and we showed that this gave a very good approximation to the moving boundary position

s for a large range of the control parameters λ and μ. Unfortunately, it was not quite so accurate for the concentration u, but a large time expansion of the resulting ODE for s gave valuable insights into how to proceed for the large time asymptotics of the full problem.

We then carried out a complete asymptotic analysis in the limits $t \to 0^+$, $t \to \infty$, $\lambda \to \infty$, $\mu = \mathcal{O}(1)$, and λ, $\mu \to \infty$. As for the related problem considered in [17], we analyzed the equations in their original form, rather than first immobilizing the boundary. This led to a systematic approach that could be applied for all the limiting expansions. The small time asymptotic solution incorporated a boundary layer at the right-hand edge, which complicated the overall structure of the approximation, and we showed that it was valid only for very small times. The large time asymptotic expansion was also complicated, due to the problem's having an equilibrium solution. We were not able to determine a closed form approximation in this limit, but after patching the unknown constant with the numerical solution, we were able to see that the expansion was accurate down to $t = \mathcal{O}(1)$. Both the small- and large time asymptotic solutions had a much richer, and much more elaborate, asymptotic structure than those of the related problem in [17], and we are confident that our approach can be applied to similar problems with initially positive moving boundary positions.

Finally, we examined the large control parameter λ expansion for two distinguished limits of the other control parameter μ: namely, $\mu \sim 1$ and $\mu \sim \lambda$. Both solutions were similar in structure, but interestingly the latter case gave much more accurate approximations at leading order. This is the more common limit to consider, and other authors often choose the spatial scaling so that $\mu = \lambda$ [10, 11]. Although we were not able to scale in the same way here, since we had an extra parameter due to $s(0)$ being nonzero, it is reassuring that our expansion for λ, $\mu \gg 1$ gave such good results, despite the fact that we could determine a closed form solution only at leading order.

REFERENCES

[1] D. Andreucci and R. Ricci, *A free boundary problem arising from sorption of solvents in glassy polymers*, Quart. Appl. Math., 44 (1987), pp. 649–657.

[2] D. Y. Arifin, L. Y. Lee, and C.-H. Wang, *Mathematical modeling and simulation of drug release from microspheres: Implications to drug delivery systems*, Adv. Drug Delivery Rev., 58 (2006), pp. 1274–1325.

[3] G. Astarita and S. Joshi, *Sample-dimension effects in the sorption of solvents in polymers—A mathematical model*, J. Membrane Sci., 4 (1978), pp. 165–182.

[4] G. Astarita and G. C. Sarti, *A class of mathematical models for sorption of swelling solvents in glassy polymers*, Polymer Engrg. Sci., 18 (1978), pp. 388–395.

[5] D. S. Cohen and T. Erneux, *Free boundary problems in controlled release pharmaceuticals. I: Diffusion in glassy polymers*, SIAM J. Appl. Math., 48 (1988), pp. 1451–1465.

[6] D. S. Cohen and C. Goodhart, *Sorption of a finite amount of swelling solvent in a glassy polymer*, J. Polymer Sci. Polymer Phys. Edn., 25 (1987), pp. 611–671.

[7] J. Crank, *The Mathematics of Diffusion*, Oxford University Press, Oxford, UK, 1956.

[8] J. Crank, *Free and Moving Boundary Problems*, Oxford University Press, New York, 1984.

[9] J. Crank and R. S. Gupta, *A moving boundary problem arising from the diffusion of oxygen in absorbing tissue*, J. Inst. Math. Appl., 10 (1971), pp. 19–33.

[10] J. D. Evans and J. R. King, *Asymptotic results for the Stefan problem with kinetic undercooling*, Quart. J. Mech. Appl. Math., 53 (2000), pp. 449–473.

[11] J. D. Evans and J. R. King, *The Stefan problem with nonlinear kinetic undercooling*, Quart. J. Mech. Appl. Math., 56 (2003), pp. 139–161.

[12] A. Fasano, G. H. Meyer, and M. Primicerio, *On a problem in the polymer industry: Theoretical and numerical investigation of swelling*, SIAM J. Math. Anal., 17 (1986), pp. 945–960.

[13] T. R. Goodman, *The heat-balance integral and its application to problems involving a change of phase*, Trans. ASME, 80 (1958), pp. 335–342.
[14] S. W. McCue, M. Hsieh, T. J. Morony, and M. I. Nelson, *Asymptotic and numerical results for a model of solvent-dependent drug diffusion through polymeric spheres*, SIAM J. Appl. Math., 71 (2011), pp. 2287–2311.
[15] S. L. Mitchell and T. G. Myers, *Application of standard and refined heat balance integral methods to one-dimensional Stefan problems*, SIAM Rev., 52 (2010), pp. 57–86.
[16] S. L. Mitchell and T. G. Myers, *Improving the accuracy of heat balance integral methods applied to thermal problems with time dependent boundary conditions*, Int. J. Heat Mass Trans., 53 (2010), pp. 3540–3551.
[17] S. L. Mitchell and S. B. G. O'Brien, *Asymptotic, numerical and approximate techniques for a free boundary problem arising in the diffusion of glassy polymers*, Appl. Math. Comp., 219 (2012), pp. 376–388.
[18] S. L. Mitchell and M. Vynnycky, *Finite-difference methods with increased accuracy and correct initialization for one-dimensional Stefan problems*, App. Math. Comp., 215 (2009), pp. 1609–1621.
[19] S. L. Mitchell, M. Vynnycky, I. G. Gusev, and S. S. Sazhin, *An accurate numerical solution for the transient heating of an evaporating droplet*, App. Math. Comp., 217 (2011), pp. 9219–9233.
[20] T. G. Myers, *Optimizing the exponent in the heat balance and refined integral methods*, Int. Comm. Heat Mass Trans., 36 (2009), pp. 143–147.
[21] T. G. Myers, *Optimal exponent heat balance and refined integral methods applied to Stefan problems*, Int. J. Heat Mass Trans., 53 (2010), pp. 1119–1127.
[22] T. G. Myers and S. L. Mitchell, *Application of the combined integral method to Stefan problems*, App. Math. Model., 35 (2011), pp. 4281–4294.
[23] N. Sadoun, E.-K. Si-Ahmed, and P. Colinet, *On the refined integral method for the one-phase Stefan problem with time-dependent boundary conditions*, App. Math. Model., 30 (2006), pp. 531–544.